Inorganic Chemistry

Article

pubs.acs.org/IC

Synthesis, Structure, and Magnetic Properties of a New Family of Tetra-nuclear $\{Mn_2^{III}Ln_2\}$(Ln = Dy, Gd, Tb, Ho) Clusters With an Arch-Type Topology: Single-Molecule Magnetism Behavior in the Dysprosium and Terbium Analogues

Vadapalli Chandrasekhar,*[,†,‡] Prasenjit Bag,[†] Manfred Speldrich,[§] Jan van Leusen,[§] and Paul Kögerler*[,§]

[†]Department of Chemistry, Indian Institute of Technology Kanpur, Kanpur-208016, India

[‡]Tata Institute of Fundamental Research, Centre for Interdisciplinary Sciences, 21 Brundavan Colony, Narsingi, Hyderabad-500075, India

[§]Institut für Anorganische Chemie, RWTH Aachen University, D-52074 Aachen, Germany

Supporting Information

ABSTRACT: Sequential reaction of Mn(II) and lanthanide(III) salts with a new multidentate ligand, 2,2′-(2-hydroxy-3-methoxy-5-methylbenzylazanediyl)diethanol ($\mathbf{LH_3}$), containing two flexible ethanolic arms, one phenolic oxygen, and a methoxy group afforded heterometallic tetranuclear complexes $[Mn_2Dy_2(LH)_4(\mu\text{-}OAc)_2](NO_3)_2\cdot 2CH_3OH\cdot 3H_2O$ (**1**), $[Mn_2Gd_2(LH)_4(\mu\text{-}OAc)_2](NO_3)_2\cdot 2CH_3OH\cdot 3H_2O$ (**2**), $[Mn_2Tb_2(LH)_4(\mu\text{-}OAc)_2](NO_3)_2\cdot 2H_2O\cdot 2CH_3OH\cdot Et_2O$ (**3**), and $[Mn_2Ho_2(LH)_4(\mu\text{-}OAc)_2]Cl_2\cdot 5CH_3OH$ (**4**). All of these dicationic complexes possess an arch-like structural topology containing a central Mn^{III}–Ln–Ln–Mn^{III} core. The two central lanthanide ions are connected via two phenolate oxygen atoms. The remaining ligand manifold assists in linking the central lanthanide ions with the peripheral Mn(III) ions. Four doubly deprotonated LH^{2-} chelating ligands are involved in stabilizing the tetranuclear assembly. A magnetochemical analysis reveals that single-ion effects dominate the observed susceptibility data for all compounds, with comparably weak Ln···Ln and very weak Ln···Mn(III) couplings. The axial, approximately square-antiprismatic coordination environment of the Ln^{3+} ions in **1**–**4** causes pronounced zero-field splitting for Tb^{3+}, Dy^{3+}, and Ho^{3+}. For **1** and **3**, the onset of a slowing down of the magnetic relaxation was observed at temperatures below approximately 5 K (**1**) and 13 K (**3**) in frequency-dependent alternating current (AC) susceptibility measurements, yielding effective relaxation energy barriers of ΔE = 16.8 cm^{-1} (**1**) and 33.8 cm^{-1} (**3**).

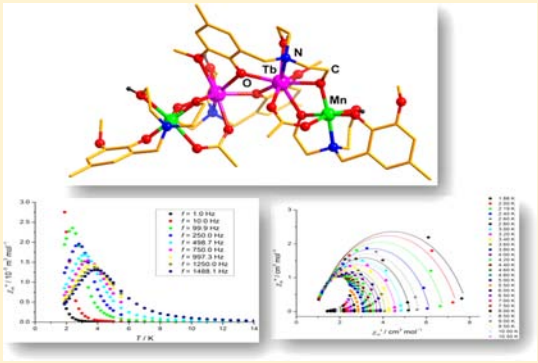

INTRODUCTION

Multimetallic architectures are attracting considerable interest for a variety of reasons including their application as models for the more complex heterogeneous metal surfaces,[1] as homogeneous catalysts,[2] and as molecular materials.[3] Most important among the multiple challenges in this area is the ability to assemble and modulate the nuclearity of such ensembles with a reasonable control on the relative disposition of the various metal ions within such architecture. Achieving this goal requires a ligand design that allows stitching together various metal ions by appropriate bridging groups. The latter is of importance in molecular magnetism, as the bridging ligands mediate the magnetic superexchange and also define the relation between the magnetic anisotropies of the spin centers.[4] Interest in single-molecule magnets (SMMs)[5] and single-chain magnets[6] continues to grow, motivated by phenomena such as quantum tunneling[7] and quantum phase interference,[8] as well as by potential applications ranging from quantum computing[9] and high-density memory storage devices[10] to magnetic refrigeration.[11] From an understanding of these systems thus far, it appears that they have to feature two important properties to function as SMMs: First, they should have a large ground-state spin; second, they also should possess a large uniaxial negative magnetic anisotropy (corresponding to a large negative zero-field splitting energy D);[12] however, there have been some examples of SMMs which possess positive D value.[13] The combination of these factors allows such systems to exhibit slow relaxation of magnetization below certain temperatures in the presence of certain applied alternating current (AC) fields. In some instances, such compounds also show hysteresis loops similar to those observed in classical magnets.[14] The importance of both S and D cannot be overemphasized; mere presence of large spin does not ensure SMM behavior. Thus, a $[Mn_{19}]$[15] complex with an S = 83/2 ground state multiplet failed to show any SMM behavior because it does not have any

Received: December 13, 2012
Published: April 24, 2013

   dx.doi.org/10.1021/ic302742u | Inorg. Chem. 2013, 52, 5035–5044

Table 1. Details of the Data Collection and Refinement Parameters for Compounds 1−4

	1	2	3	4
formula	$C_{58}H_{96}Mn_2Dy_2N_6O_{31}$	$C_{58}H_{96}Mn_2Gd_2N_6O_{32}$	$C_{62}H_{99}Mn_2Tb_2N_6O_{31}$	$C_{61}H_{105}Cl_2Ho_2Mn_2N_4O_{25}$
M/g mol^{-1}	1808.29	1813.79	1852.19	1802.11
crystal system	triclinic	triclinic	triclinic	monoclinic
space group	$P\bar{1}$	$P\bar{1}$	$P\bar{1}$	$P2_1/c$
wavelength (MoK$_\alpha$)/Å	0.71069	0.71069	0.71069	0.71069
unit cell dimensions				
a/Å	15.243(5)	15.268(5)	15.246(5)	15.665(5)
b/Å	15.813(5)	15.808(5)	15.802(5)	32.486(5)
c/Å	17.963(5)	17.965(5)	17.911(5)	15.691(5)
α/deg	66.685(5)	66.994(5)	66.852(5)	90.000(5)
β/deg	82.697(5)	82.487(5)	82.714(5)	108.600(5)
γ/deg	70.871(5)	70.931(5)	71.074(5)	90.000(5)
V/Å^3	3757(2)	3772(2)	3753(2)	7568(4)
Z	2	2	2	4
ρ_c/ g cm^{-3}	1.599	1.615	1.639	1.584
μ/mm^{-1}	2.379	2.149	2.278	2.540
F(000)	1832	1840	1882	3668
crystal dimension/mm^3	0.14 × 0.11 × 0.085	0.13 × 0.11 × 0.08	0.125 × 0.10 × 0.075	0.13 × 0.11 × 0.09
θ range/deg	1.70−25.50	1.88−26.00	2.25−25.50	1.86−25.50
limiting indices	$-12 \le h \le 18$	$-18 \le h \le 18$	$-18 \le h \le 18$	$-16 \le h \le 18$
	$-18 \le k \le 19$	$-17 \le k \le 19$	$-18 \le k \le 19$	$-39 \le k \le 38$
	$-21 \le l \le 20$	$-22 \le l \le 22$	$-14 \le l \le 21$	$-17 \le l \le 19$
reflns collected	20246	21153	19908	40300
independent reflns	13663 (R_{int} = 0.0325)	14478 (R_{int} = 0.0348)	13614 (R_{int} = 0.0529)	14027 (R_{int} = 0.0765)
completeness to θ	97.6%	97.7%	97.3%	99.7%
refinement method	full-matrix least-squares on F^2	full-matrix least-squares on F^2	full-matrix least-squares on F^2	full-matrix least-squares on F^2
data/restraints/params	13663/39/915	14478/47/937	13609/49/959	14027/13/897
goodness-of-fit on F^2	1.052	1.045	1.073	1.039
final R indices	R_1 = 0.0659,	R_1 = 0.0693	R_1 = 0.0925	R_1 = 0.0579
[$I > 2\theta(I)$]	wR_2 = 0.1694	wR_2 = 0.1852	wR_2 = 0.2285	wR_2 = 0.1543
R indices (all data)	R_1 = 0.0823,	R_1 = 0.0897,	R_1 = 0.1202,	R_1 = 0.0840,
	wR_2 = 0.1888	wR_2 = 0.2119	wR_2 = 0.2483	wR_2 = 0.1771
$\rho_{max/min}$ (e·Å^{-3})	3.190 and −1.589	3.800 and −2.054	3.999 and −1.934	3.028 and −1.163

appreciable D value. On the other hand, replacing the central Mn^{2+} ion with a Dy^{3+}ion gave a Mn_9−Dy−Mn_9 complex[16] which exhibited SMM behavior because of its significant molecular magnetic anisotropy. Thus, complexes containing 3d and 4f metal ions are of interest as well as those where single-ion anisotropy can be realized; note however that the zero-field splitting of the M_J states in 4f complexes exhibiting slow relaxation of the magnetization usually do not result in a simple parabola (as seen for 3d-based SMMs) between the energetically lowest M_J states but in more complex patterns with multiple maxima and minima. In this context, many 3d/4f systems have been investigated; particularly those that contain Cu^{2+}/$Ln^{3+}$and Ni^{2+}/Ln^{3+} systems.[17,18] Among the Mn^{3+}/Ln^{3+} systems several high-nuclearity clusters are known: $Mn_{21}Dy$,[19a] $Mn_{12}Gd$,[19b] $Mn_{11}Gd_2$,[19c] Mn_6Dy_6,[19d] Mn_5Ln_4,[19e] Mn_9Dy_8,[19f] $Mn_{11}Dy_4$,[19g] Mn_4Ln_4,[20] Mn_2Ln_2,[21] Mn_5Ln_6,[22a] Mn_2Ln_3,[22b] Mn_6Ln_2,[22c] $Mn_{12}Dy_6$,[22d] Mn_4Ln_2.[23] Interestingly, low-nuclearity aggregates are quite rare.[24] We have recently reported a series of Mn_2Ln compounds using a phosphorus-supported tris-hydrazone ligand.[25]Among Mn_2-Ln_2 complexes, only three examples are thus far known.[21] Recognizing that assembling a tetranuclear aggregate containing two Mn^{3+} and two Ln^{3+} ions requires the design of a chelating, flexible, and sterically unencumbered ligand system, we have designed a new multidentate ligand, 2,2′-(2-hydroxy-3-methoxy-5-methylbenzylazanediyl)diethanol (**LH_3**), which contains two flexible ethanolic arms, one phenolic oxygen, and a methoxy group at the neighboring carbon of the phenolic oxygen. This ligand design is based on a modification of a ligand type that has been reported in literature earlier for the preparation of a divanadium(III) complex.[26] Based on this ligand system, we herein report the synthesis, characterization, and detailed magnetic properties of a series of isostructural heterometallic tetranuclear {$Mn^{III}_2Ln_2$} complexes [Ln = Dy (**1**), Gd (**2**), Tb (**3**), Ho (**4**)]. Among the known tetranuclear {$Mn^{III}_2Ln_2$} complexes, compounds **1**−**4** represent a new structural type. Interestingly, compounds **1** and **3** exhibit SMM characteristics.

EXPERIMENTAL SECTION

Reagents and General Procedures. Solvents and other general reagents used in this work were purified according to standard procedures.[27] 2-Methoxy-4-methylphenol (Sigma Aldrich, U.S.A.) was used as purchased. Diethanolamine, paraformaldehyde, and Mn(OAc)$_2$·4H$_2$O were obtained from SD Fine Chemicals, Mumbai, India, and were used as such. LnX_3·nH_2O (X = NO_3 for **1**−**3**; X = Cl for **4**) were obtained from Aldrich Chemical Co. and were used as such.

Syntheses. *2,2′-(2-Hydroxy-3-methoxy-5-methylbenzylazanediyl)diethanol (LH_3).*[26] The synthesis of LH_3 was carried out by adapting a literature procedure.[26] To a stirred solution of 2-methoxy-4-methylphenol (6.0 g, 43.0 mmol), diethanolamine (4.52 g, 43.0 mmol) in dry methanol (40 mL) and paraformaldehyde (1.93 g, 64.5 mmol) were added, and the solution was refluxed under a dry nitrogen atmosphere for 3 days. After this, the solution was evaporated to dryness under vacuum, and the resulting

dx.doi.org/10.1021/ic302742u | Inorg. Chem. 2013, 52, 5035−5044

Scheme 1. Synthesis of Compounds 1−4[a]

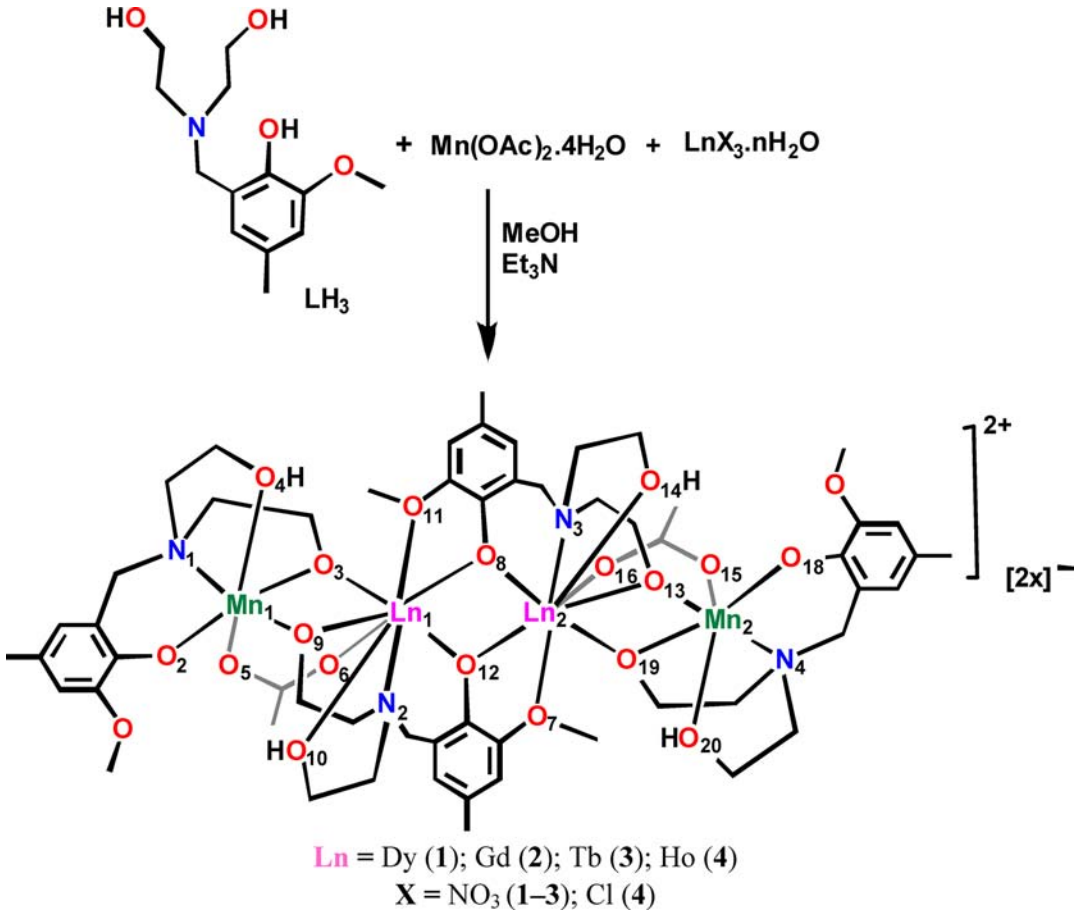

[a]Atom numbering applicable to compound **1**.

crude oily mixture was purified by column chromatography on silica gel (5:95 methanol/ethyl acetate) to afford LH_3 as a pale yellow solid. Yield: 9.30 g (84.50%). Mp: 60 °C. FT-IR (KBr), cm^{-1}: 3324 (b), 2930 (m), 2919 (m), 1600 (s), 1499 (s), 1457 (s) 1396 (m), 1367 (s), 1243 (s), 1155 (s), 1089 (s). ^1H NMR ($CDCl_3$, δ, ppm): 6.55 (s, 1H, Ar−H), 6.37 (s, 1H, Ar−H), 3.78 (s, 3H, OCH_3), 3.75 (s, 2H, $ArCH_2$), 3.64 (t, 4H, CH_2O), 2.69 (t, 4H, NCH_2), 2.17 (s, 3H, $ArCH_3$). ESI-MS (m/z): 256.15 (M^+). C/H/N analysis, calcd.for $C_{13}H_{21}NO_4$: C, 61.16; H, 8.29; N, 5.49%. Found: C, 61.02; H, 8.11; N, 5.30%.

*Preparation of the Tetranuclear Complexes **1**−**4**.* A general protocol was applied for the preparation of all the metal complexes (**1**−**4**) as follows: LH_3 (0.102 g, 0.40 mmol) was dissolved in methanol (20 mL). $Ln(NO_3)_3{\cdot}nH_2O$ (0.20 mmol) (for the preparation of **1**−**3**) and triethylamine (0.06 mL, 0.40 mmol) were added to this solution. The reaction mixture was stirred for 1 h. At this stage, $Mn(OAc)_2{\cdot}4H_2O$ (0.049 g, 0.20 mmol) was added, and the reaction mixture was stirred for a further period of 1.5 h at 20 °C to afford a clear solution. A deep green-colored solution was obtained which was stripped off its solvent in vacuo resulting in a green solid which was washed with diethyl ether and dried affording pure samples of **1**−**3**. For the preparation of **4**, $HoCl_3{\cdot}6H_2O$ was used as the lanthanide salt. X-ray quality dark green crystals of **1**−**4** were grown by vapor diffusion of diethyl ether into the methanolic solution of the corresponding complex. The characterization data for these complexes are given below.

*$[Mn_2Dy_2(LH)_4(\mu\text{-}OAc)_2](NO_3)_2{\cdot}2CH_3OH{\cdot}3H_2O$ (**1**).* Yield: 0.080 g (44.4% based on Dy). Mp: >220 °C. IR (KBr), cm^{-1}: 3132 (b), 2978 (m), 2919 (m), 2853 (m), 1558 (s), 1489 (s), 1420 (m), 1384 (s), 1253 (s), 1156 (s), 1064 (s). ESI-MS m/z, ion: 783.13, $[M]^{2+}$. C/H/N analysis, calcd. for $C_{58}H_{96}N_6O_{31}Mn_2Dy_2$ (1808.29 g mol^{-1}): C, 38.52; H, 5.35; N, 4.65%. Found: C, 38.20; H, 5.04; N, 4.48%.

*$[Mn_2Gd_2(LH)_4(\mu\text{-}OAc)_2](NO_3)_2{\cdot}2CH_3OH{\cdot}3H_2O$ (**2**).* Yield: 0.065 g (35.8% based on Gd). Mp: >220 °C. IR (KBr), cm^{-1}: 3189 (b), 2974 (m), 2915 (m), 2861 (m), 1558 (s), 1488 (s), 1420 (m), 1384 (s), 1254 (s), 1156 (s), 1073 (s). ESI-MS m/z, ion: 778.13, $[M]^{2+}$. C/H/N analysis, calcd. for $C_{58}H_{96}N_6O_{32}Mn_2Gd_2$ (1813.79 g mol^{-1}): C, 38.41; H, 5.33; N, 4.63%. Found: C, 38.15; H, 5.09; N, 4.41%.

*$[Mn_2Tb_2(LH)_4(\mu\text{-}OAc)_2](NO_3)_2{\cdot}2H_2O{\cdot}2CH_3OH{\cdot}Et_2O$ (**3**).* Yield: 0.076 g (41.03% based on Tb). Mp: >220 °C. IR (KBr), cm^{-1}: 3173 (b), 2977 (m), 2920 (m), 2852 (m), 1557 (s), 1488 (s), 1420 (m), 1384 (s), 1254 (s), 1155 (s), 1064 (s). ESI-MS m/z, ion: 779.12, $[M]^{2+}$. C/H/N analysis, calcd. for $C_{62}H_{99}N_6O_{31}Mn_2Tb_2$(1852.19 g mol^{-1}): C, 40.20; H, 5.39; N, 4.54%. Found: C, 39.85; H, 5.11; N, 4.36%.

*$[Mn_2Ho_2(LH)_4(\mu\text{-}OAc)_2]Cl_2{\cdot}5CH_3OH$ (**4**).* Yield: 0.079 g (42.5% based on Ho). Mp: >220 °C. IR (KBr), cm^{-1}: 3392 (b), 2971 (w) 2914 (m), 2862 (m), 1560 (s), 1489 (s), 1422 (m), 1360 (s), 1255 (s), 1157 (s), 1069 (s). ESI-MS m/z, ion: 785.12, $[M]^{2+}$. C/H/N analysis, calcd. for $C_{61}H_{105}N_4O_{25}Cl_2Mn_2Ho_2$ (1852.19 g mol^{-1}): C, 40.59; H, 5.86; N, 3.10%. Found: C, 40.12; H, 5.53; N, 2.90%.

Instrumentation. Melting points were measured using a JSGW melting point apparatus and are uncorrected. IR spectra were recorded as KBr pellets on a Bruker Vector 22 FT-IR spectrophotometer operating at 400−4000 cm^{-1}. ^1H NMR spectra were recorded on a JEOL-JNM LAMBDA model 400 spectrometer using $CDCl_3$ operating at 400 MHz. Elemental analyses of the compounds were obtained from Thermoquest CE instruments CHNS-O, EA/110 model. Electrospray ionization mass spectrometry (ESI-MS) spectra were recorded on a Micromass Quattro II triple quadrupole mass spectrometer. Methanol was used as the solvent for the electrospray

dx.doi.org/10.1021/ic302742u | *Inorg. Chem.* 2013, 52, 5035−5044

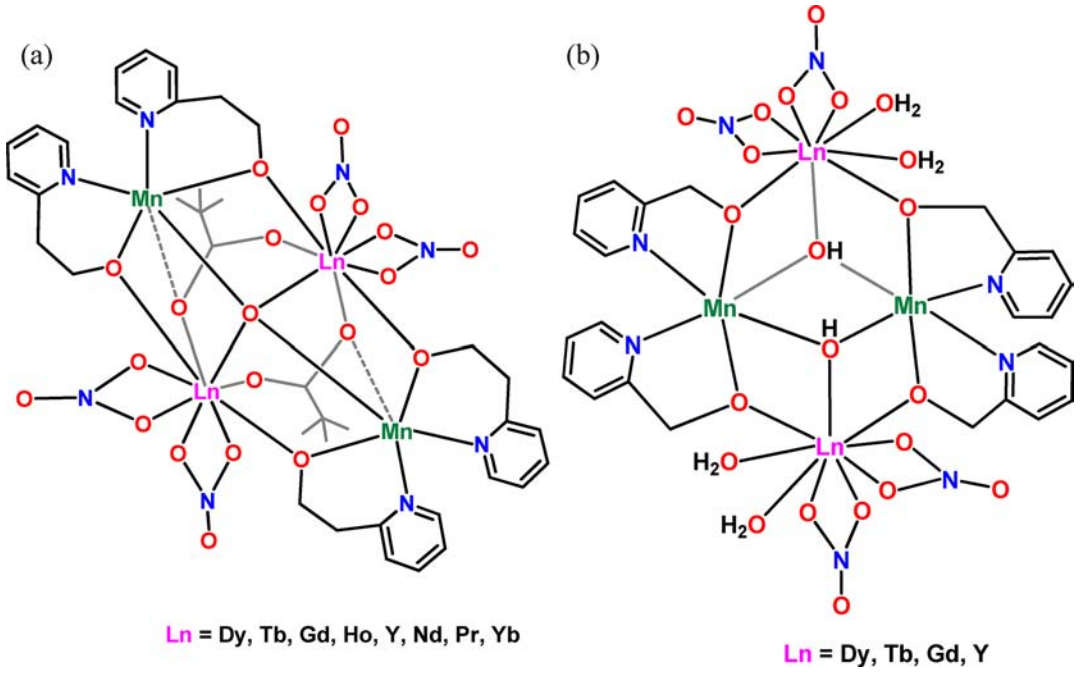

Figure 1. Some earlier-known examples of $Mn_2(III)Ln_2$ compounds.[21b,c] The left example contains pivalate ligands which bind the two central lanthanide ions along with a terminal manganese ion. The example on the right is a carboxylate-free system and contains μ_3-OH ligands that bridge the central manganese ions along with a terminal lanthanide ion.

ionization (positive ion, full scan mode). Capillary voltage was maintained at 2 kV, and cone voltage was kept at 31 kV.

X-ray Crystallography. The crystal data and the cell parameters for **1**−**4** are given in Table 1. The crystal data for **1**−**4** have been collected on a Bruker AXS SMART APEX CCD X-ray diffractometer using a Mo sealed-tube X-ray source. The program SMART[28a] was used for collecting frames of data, indexing reflections, and determining lattice parameters, SAINT[28a] for integration of the intensity of reflections and scaling, SADABS[28b] for absorption correction, and SHELXTL[27c,d] for space group and structure determination and least-squares refinements on F^2. All structures were solved by direct methods using the programs SHELXS-97[28e] and refined by full-matrix least-squares methods against F^2 with SHELXL-97.[28e] Hydrogen atoms were fixed at calculated positions, and their positions were refined by a riding model. All non-hydrogen atoms were refined with anisotropic displacement parameters. The crystallographic figures used in this manuscript have been generated using Diamond 3.1e software.[28f] The high R_1 = 0.0925 for compound **3** is likely due to the small crystal size, disordered water molecules, and a Q′ peak value of 3.9 around Tb1; despite several tries, we were not able to obtain better crystals.

Magnetochemistry. Both direct current (DC) and alternating current (AC) susceptibility data were recorded using a Quantum Design MPMS-5XL SQUID magnetometer. Microcrystalline samples were pressure-compacted and immobilized into cylindrical PTFE sample holders. DC susceptibility data was acquired as a function of temperature (2.0−290 K) at 0.1 T and, for compound **2**, as a function of the applied magnetic field (0.1−5.0 T) at 2.0 T. AC susceptibility data were determined in the 0.1−1500 Hz frequency range (T = 1.9−20 K, H_{ac} = 3 G), in the absence of a static bias field. Only compounds **1** and **3** exhibited significant out-of-phase components above 2.0 K; a small DC bias field (10 G) did not significantly affect the AC susceptibility for these compounds. Experimental magnetic data were corrected for diamagnetic contributions calculated from tabulated values. Note that all quantities are given in SI units. The magnetic data was processed using the computational framework CONDON,[29] which allows to reproduce both intramolecular exchange coupling and single ion effects: interelectronic repulsion (H_{ee}), spin−orbit coupling (H_{so}), ligand-field effect (H_{lf}), and the Zeeman effect of an applied field (H_{mag}), see Supporting Information for details. Intramolecular exchange between magnetic centers was modeled using the Heisenberg−Dirac−van Vleck approach assuming only nearest-neighbor interactions (i.e., a Mn−Ln−Ln−Mn connectivity), $H_{ex} = -2(J_1(\hat{S}_{Ln^{3+}}\cdot\hat{S}_{Ln^{3+}}) + J_2(\hat{S}_{Ln^{3+}}\cdot\hat{S}_{Mn3+}))$.

RESULTS AND DISCUSSION

Synthetic Aspects. The multisite coordinating ligand, LH_3, was prepared by a one-pot synthesis involving the reaction of 2-methoxy-4-methylphenol, diethanolamine, and paraformaldehyde. The ligand LH_3, is based on a basic phenol-framework and contains two unsymmetrically disposed substituents. Adjacent to the phenol unit on one side is a diethanolamine group and on the other side a methoxy group (Scheme 1). Thus, a total of five coordination sites are available: one nitrogen, one phenolate oxygen, two alkoxy (or -CH_2OH units) and one methoxy oxygen atoms. Among these, the weakly coordinating methoxy group can specifically bind to the lanthanide ions. The flexible diethanolamine arms of the ligand containing three coordination sites, along with the phenolate oxygen atom, can effectively bridge different metal centers. In accordance with this expectation, LH_3 reacts with $Mn(OAc)_2\cdot 4H_2O$ and $LnX_3\cdot nH_2O$ (in a 2:1:1 stoichiometric ratio, in the presence of triethylamine as the base) in methanol affording the heterometallic tetranuclear dicationic complex salts $[(LH)_4(AcO)_2Mn_2Ln_2]X_2$ (**1**−**4**) in good yields (Scheme 1; see the Experimental Section for details of syntheses). The formation of these complexes is depicted in eq 1.We believe that aerial oxygen is responsible for the oxidation of Mn(II) to Mn(III) under the basic reaction conditions provided by Et_3N. The molecular structures of all four complexes were determined by single-crystal X-ray crystallography (vide infra). Compounds **1**−**4** retain their molecular integrity in solution as evidenced by the detection of their molecular ion peaks in their ESI-MS spectra (see Experimental Section; see also Supporting Information, Figures S2−S5). It is interesting to note that the preparation of two of the previously known Mn_2Ln_2 complexes used either (2-hydroxymethyl)pyridine or

dx.doi.org/10.1021/ic302742u | Inorg. Chem. 2013, 52, 5035−5044

(2-hydroxyethyl)pyridine as the ligands; one of these was carboxylate-free while the other also contained pivalate ligands[21b,c] (Figure 1). The third previously known Mn_2Ln_2 complex was prepared using 2-ethyl-2-(hydroxymethyl)-propane-1,3-diol.[21a]

$$2Mn(OAc)_2 + 2Ln(NO_3)_3 + 4LH_3 + 4Et_3N + 0.5O_2 \rightarrow [Mn^{III}_2Ln_2(LH)_4(\mu\text{-}OAc)_2](NO_3)_2 + 2CH_3CO_2H + 4Et_3NHNO_3 + H_2O \quad (1)$$

X-ray Crystallography. Single-crystal X-ray study reveals that the compounds **1**−**3** crystallize in the space group $P\bar{1}$ while **4** crystallizes in $P2_1/c$. All the compounds are dicationic in nature and have the same structural topology with an arch-like central tetrametallic core where the Mn(III) ions are present in the periphery and the lanthanide ions in the center (Figures 2 and 3). In view of the similarity of the molecular structures of **1**−**4**, we describe the structure of $[(LH)_4Mn_2Dy_2]^{2+}$ (**1**) as a representative example. The structural features of this compound are detailed in Figures 2−4. Selected bond parameters of **1** are summarized in Table 2. The molecular structures and selected bond parameters of the other compounds are given in the Supporting Information, Figures S6−S8, Tables S2−S4.

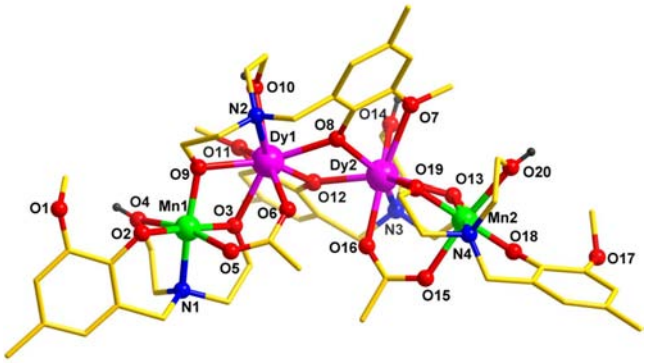

Figure 2. Molecular structure of **1**; hydrogen atoms, counteranions, and solvent molecules were omitted for clarity.

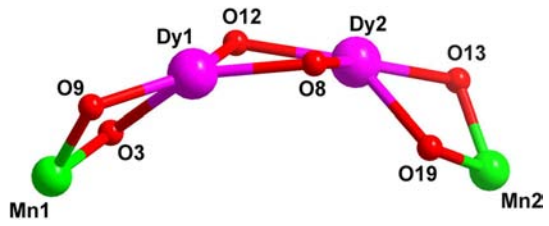

Figure 3. View of the arch-type topology of central Mn_2Dy_2 core. Selected bond distances (Å) and bond angles (deg): Mn(1)−O(9) = 1.918(8), Mn(1)−O(3) = 1.902(7), Dy(1)−O(8) = 2.315(7), Dy(1)−O(12) = 2.326(7), Dy(1)−O(9) = 2.304(7), Dy(1)−O(3) = 2.359(7), Dy(1)−O(8) = 2.315(7), Dy(1)−O(12) = 2.326(7), Dy(2)−O(19) = 2.343(7), Dy(2)−O(13) = 2.300(7), Mn(2)−O(13) = 1.923(7), Mn(2)−O(19) = 1.900(7), Dy(1)−Mn(1) = 3.301(2), Dy(1)−Dy(2) = 3.712(1) Dy(2)−Mn(2) = 3.297(2), Mn(1)−O(3)−Dy(1) = 101.0(3), Mn(1)−O(9)−Dy(1) = 102.5(3), Mn(2)−O(19)−Dy(2) = 101.3(3), Mn(2)−O(13)−Dy(2) = 102.1(3), Dy(2)−O(12)−Dy(1) = 106.2(3), Dy(2)−O(8)−Dy(1) = 106.8(3), Mn(1)−Dy(1)−Dy(2) = 133.88(4), Mn(2)−Dy(2)−Dy(1) = 133.71(4).

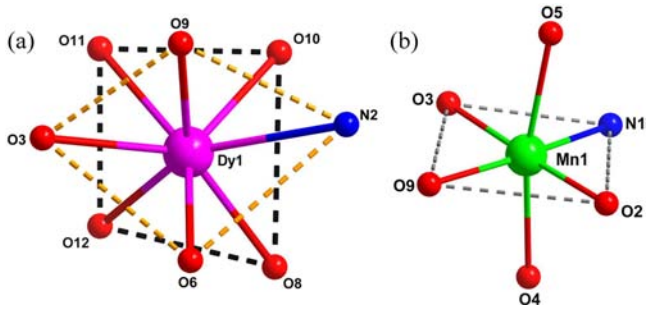

Figure 4. (a) Distorted square antiprismatic coordination geometry of the dysprosium(III) ions in **1**. (b) Distorted octahedral environment around the manganese(III) ions in **1**.

Of the four ligands involved in the assembly of **1**, two are present as terminal ligands and two others in the center. Each of the two centrosymmetrically related terminal ligands binds to a Mn(III) ion through the phenolate oxygen (O18), the amino nitrogen (N4), a deprotonated $[CH_2-CH_2-O]^-$ arm (O19), and the alcoholic $[CH_2-CH_2-OH]$ group (O20). The protonation state of the alkoxy oxygen was determined through a bond valence sum (BVS) calculation of O atoms (Supporting Information, Table S2).[30] The BVS value of about 1.1 suggests that O4, O10, O14, and O20 are monoprotonated, while the corresponding value of about 2.0 for O3, O9, O13 and O19 confirms their deprotonated state. The oxygen atom of the deprotonated arm, O19, also bridges the terminal manganese ion (Mn2) and the central dysprosium ion (Dy2). The coordination environment around Mn2 is completed by an oxygen atom of the bridging acetate group (which binds Dy2 and Mn2) and O13 which also bridges Mn2 with Dy2. The two central ligands are involved, principally, in holding the two dysprosium ions (Dy1 and Dy2) together, apart from bridging one of the terminal manganese ions. Thus, each of the two central ligands, also doubly deprotonated like the terminal ligands, bridge Dy1 and Dy 2 through the phenolate oxygen atom (O8). While the methoxy arm of the ligand (O11) binds to Dy1, the amino nitrogen binds to Dy2. One of the flexible $-CH_2CH_2OH$ arms (O14) binds to a dysprosium (Dy2) while the other, the deprotonated counterpart, $[-CH_2-CH_2-O]^-$ (O13) bridges Dy2 with Mn2. Finally, the acetate ligand, which is present as an η^1-η^1 bridging ligand (O15 and O16), bridges Dy2 with Mn2. Thus, while Dy(III) and Mn(III) are bridged by two oxygen atoms emanating from two flexible arms of two different LH^{2-} ligands (CH_2CH_2O and CH_2CH_2OH) and one μ-OAc group, the two central Dy(III) ions are bridged by only two phenolate oxygen atoms. This cumulative coordination action results in three contiguous four-membered rings: two terminal heterometallic $MnDyO_2$ rings and one central Dy_2O_2 ring. The two dysprosium ions, Dy1 and Dy2 form the spirocyclic centers of two four-membered rings each. The overall topology of this interconnected multi-ring system is arch-shaped (Figure 3) which is quite distinct and different from the tetranuclear Mn_2Ln_2 derivatives known in literature,[21] thus far.

The two manganese ions, Mn1 and Mn2 are in the +III oxidation state, as evidenced from their characteristically axially elongated octahedral MnO_5N coordination geometries with the Jahn−Teller axes along O4−Mn1−O5 and O15−Mn2−O20, respectively, with axial bond lengths of Mn1−O5, 2.204(8) and

dx.doi.org/10.1021/ic302742u | Inorg. Chem. 2013, 52, 5035−5044

Table 2. Selected Bond Distances (Å) and Bond Angles (deg) for Compound 1

bond lengths around manganese(1)		bond lengths around manganese(2)			
Mn(1)−N(1)	2.076(9)	Mn(2)−N(4)	2.057(9)	Mn(1)−O(3)−Dy(1)	101.0(3)
Mn(1)−O(2)	1.860(8)	Mn(2)−O(18)	1.872(7)	Mn(1)−O(9)−Dy(1)	102.5(3)
Mn(1)−O(3)	1.902(7)	Mn(2)−O(13)	1.923(7)	Dy(2)−O(12)−Dy(1)	106.2(3)
Mn(1)−O(9)	1.918(8)	Mn(2)−O(19)	1.900(7)	Dy(2)−O(8)−Dy(1)	106.8(3)
Mn(1)−O(4)	2.298(8)	Mn(2)−O(15)	2.202(8)	Mn(2)−O(19)−Dy(2)	101.3(3)
Mn(1)−O(5)	2.204(8)	Mn(2)−O(20)	2.287(9)	Mn(2)−O(13)−Dy(2)	102.1(3)
				Mn(1)−Dy(1)−Dy(2)	133.88(4)
				Mn(2)−Dy(2)−Dy(1)	133.71(4)
bond lengths around dysprosium(1)		bond lengths around dysprosium(2)			
Dy(1)−N(2)	2.574(9)	Dy(2)−O(16)	2.286(8)		
Dy(1)−O(3)	2.359(7)	Dy(2)−O(7)	2.485(7)		
Dy(1)−O(6)	2.299(8)	Dy(2)−O(8)	2.309(7)		
Dy(1)−O(8)	2.315(7)	Dy(2)−O(12)	2.314(7)		
Dy(1)−O(9)	2.304(7)	Dy(2)−O(13)	2.300(7)		
Dy(1)−O(10)	2.369(8)	Dy(2)−O(14)	2.380(8)		
Dy(1)−O(11)	2.488(7)	Dy(2)−N(3)	2.600(8)		
Dy(1)−O(12)	2.326(7)	Dy(2)−O(19)	2.343(7)		

Mn1−O4, 2.298(8) Å that are much longer than the equatorial bond lengths, Mn1−O2, 1.860(8), Mn1−O3, 1.902(7), and Mn1−O9, 1.918(8) Å (Figure 4). The BVS calculations (Supporting Information, Table S1) also support the assignment of an oxidation state of +III to the manganese ions.[30] The two central dysprosium ions reside in distorted square-antiprismatic DyO_7N environments (Figure 4). The Dy−O bond distances are, as anticipated, longer than the Mn−O bond distances. Unlike the Mn−O bond distances, the Dy−O bond distances are nearly similar (average: 2.351(8) Å) with the shortest distance of 2.299(8) Å for the Dy1−O6 bond involving the acetate oxygen, and the longest distance of 2.488(7) Å involving the methoxy oxygen (Dy1−O11). The intramolecular intermetallic distances involved are Mn···Dy, 3.300 Å, and Dy···Dy, 3.712 Å (Table 2). The crystal structure of **1** reveals the formation of a supramolecular polymeric one-dimensional (1D) chain through intermolecular O−H·····O interactions (Supporting Information). The hydrogen bond parameters involved in these interactions are tabulated in Supporting Information, Table S5.

Magnetism. The low-field magnetic DC susceptibility data for compounds **1**−**4** exhibit clear signatures of single-ion effects and weak Ln···Mn as well as very weak Ln···Ln antiferromagnetic exchange couplings. To reproduce these data, common coordination environments are assumed for all Ln^{3+} sites (square-antiprismatic, see Figure 4a) and all Mn^{3+} (tetragonally elongated with idealized D_{4h} symmetry, see Figure 4b).

Compound **2**: The $4f^7/3d^4$ system with the free-ion ground terms $^8S_{7/2}$ and $^5D_0$ shows a nearly temperature independent effective Bohr magneton number of 13.2 (2 × Gd^{3+} and 2 × Mn^{3+} ions) down to about 150 K, and χ^{-1}; M vs T remains linear between 50 and 290 K. Taken as a spin-only system, a least-squares fit to a Curie−Weiss expression yields a Weiss temperature $\theta_a = -9.4$ K, that is, a global parameter accounting for all coupling interactions in **2**. The full temperature range is successfully reproduced (SQ = 0.62%) when both exchange coupling as well as single-ion effects (Table 3) are taken into account (Figure 5). Within the tetranuclear complex in **2**, the

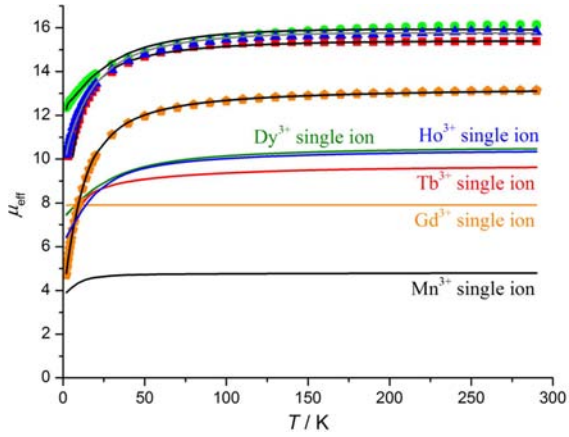

Figure 5. Temperature dependence of μ_{eff} at 0.1 T for compounds **1**−**4** as well as simulated curves for single Mn^{3+} and Ln^{3+} ions in their idealized coordination environments. Solid symbols: experimental data (green circles: **1**; orange pentagons: **2**; red squares: **3**; blue triangles: **4**); solid graphs: least-squares fits (black or gray) and simulated single-ion contributions (individually labeled).

Gd···Gd contact (ca.3.75 Å) is characterized by $J_1 = -0.07$ cm^{-1}, and the two shorter (ca. 3.31 Å) Gd···Mn contacts result in $J_2 = -1.14$ cm^{-1}, in line with the fact that Ln···Ln ($|J_{ex}| \leq 1.0$ cm^{-1}) interactions are usually 1 order of magnitude smaller than Ln···3d ($|J_{ex}| \leq 10$ cm^{-1}) interactions. This weak antiferromagnetic interaction is also well-documented for, for example, dialkoxide-bridged Mn···Gd[23b,24c] and diphenoxo-bridged Gd···Gd[31] systems. Note that these J_1 and J_2 values correspond to a Weiss temperature of $\theta_b = -9.14$ K in the high-temperature expansion limit, in good agreement with the directly derived value; the small negative residual $\theta_a - \theta_b = -0.26$ K likely corresponds to weak antiferromagnetic intercluster coupling between neighboring $\{Mn_2Gd_2\}$ entities, potentially mediated by both intercluster hydrogen bonds and dipole−dipole coupling.

In contrast to the spin-only ($S = 7/2$) Gd(III)-based **2**, the lanthanide(III) ions in compounds **1**, **3**, and **4** in their idealized

dx.doi.org/10.1021/ic302742u | Inorg. Chem. 2013, 52, 5035−5044

Table 3. Magnetochemical Analysis Details

		2	3	1	4
magnetic center	$Mn^{3+}(3d^4)$	Gd^{3+} ($4f^7$)	Tb^{3+} ($4f^8$)	Dy^{3+} ($4f^9$)	Ho^{3+} ($4f^{10}$)
$F^2(B)/cm^{-1}$		91800	97650	94500	101250
$F^4(C)/cm^{-1}$		64425	68530	66320	71057
F^6/cm^{-1}		49258	52397	50706	54328
ζ/cm^{-1}		1470	1705	1932	2163
μ_{eff} (300 K)		13.19	14.62	16.13	15.89
θ_a/K (50–290 K)		−9.4			
$C/10^{-4}$ cm^3 K mol^{-1}		2.734			
B^2_0/cm^{-1}	−4500		−30	190	370
B^4_0/cm^{-1}	14900		−3710	−3940	−4110
$B^4_0/$ cm^{-1}	7500				
$B^6_0/$ cm^{-1}			105	195	301
J_1 /cm^{-1} (Ln^{3+}–Ln^{3+})		−0.05	0.02	0.08	0.06
J_2 /cm^{-1} (Ln^{3+}–Mn^{3+})		−1.05	−0.23	−0.05	−0.11
SQ^a/%		0.7	1.07	1.17	0.9
$\chi_{dia}/$ 10^{-10}m^3 mol^{-1}		−110.16	−110.16	−110.16	−110.16

^{a}Quality of Fit: $SQ=\{(\sum_{i=1}^{n}[(\chi_i^{obs}-\chi_i^{calc})/\chi_i^{obs}]^2)(1/n)\}^{1/2}$.

D_{4d}-symmetric environments are strongly influenced by ligand-field effects and spin–orbit coupling. Thus, modeling the temperature-dependent magnetic moment of **1**, **3**, and **4** requires accounting for all single-ion effects, whereby the ligand field parameters determined for **2**, as well as standard values for the spin–orbit coupling constants and the Slater–Condon parameters F^2, F^4, and F^6, are used as constants in the fitting of the compounds to avoid overparametrization. In **1**, **3**, and **4**, the Mn···Ln coupling was found to be weakly antiferromagnetic, whereas the Ln···Ln coupling is very weakly ferromagnetic (Table 3).

The single-ion effects on the ground state multiplets for Tb^{3+} (**3**), Dy^{3+} (**1**), and Ho^{3+} (**4**) derived from the susceptibility fits translate into the characteristic zero-field splitting of the J ground states into the corresponding m_J substates (Figure 6a). Note that the linear dependency of B^2_0, B^4_0, and B^6_0 on the number of f electrons, going from Tb^{3+} to Dy^{3+} to Ho^{3+}, is due to the increase of the effective nuclear charge of these ions (Figure 6b). To determine if these splitting patterns lead to an effective slowing-down of the relaxation of the magnetization upon an external field change, that is, one of the fundamental characteristics of single-molecule magnets, AC susceptibility measurements were performed. Only the Dy^{3+}-based compound **1** and the Tb^{3+}-based compound **3** were found to exhibit significant slow relaxation above 1.9 K (Supporting Information, Figure S10 and S11). For each temperature, the corresponding AC susceptibility data (the in-phase component χ' and the out-of-phase component χ'') can be fitted to a Cole–Cole equation (Figure 7). The resulting temperature-dependent fit parameters allow the determination of the average relaxation times of the magnetization, τ, on the basis of an Arrhenius expression, $\tau = \tau_0 \exp(\Delta E/k_BT)$ (Supporting Information, Figure S1).[32] This results in the effective energy barriers ΔE = 16.8 (±0.8) cm^{-1} (**1**) and ΔE = 33.8 (±2.8) cm^{-1} (**3**), as well as the time constants $\tau_0 = 8.30 \times 10^{-9}$ (±2.94 × 10^{-9}) s (**1**) and $\tau_0 = 1.63 \times 10^{-8}$ (±1.00 × 10^{-8}) s (**3**). The distribution width of τ is quantified by the scalar parameter α in the generalized Debye model, where a deviation from α = 0 indicates multiple relaxation times due to multiple relaxation mechanisms. The corresponding values α = 0.1918 (±0.0693) (**1**) and α = 0.1175 (±0.0669) (**3**), averaged over all isotherms, thus show that several relaxation mechanisms exist. We note that the observed relaxation phenomena are not only related to the zero-field splitting of the m_J states of the Ln^{3+} centers, but are in part also influenced by the magnetic anisotropy of the Jahn–Teller-distorted Mn^{3+} centers. The fact that the anisotropy axes of the individual Ln^{3+} and the Jahn–Teller axes of the Mn^{3+} ions are not oriented in a collinear fashion because of the arch-type shape of the Mn–Ln–Ln–Mn backbone reduces the effective energy barriers that are significantly smaller than the overall ligand field splitting of the individual Tb^{3+} and Dy^{3+} ions in **3** and **1**. The arch-type geometry of these complexes could potentially also cause local stray fields that increase the transition probabilities of underlying nonthermal relaxation mechanisms such as quantum

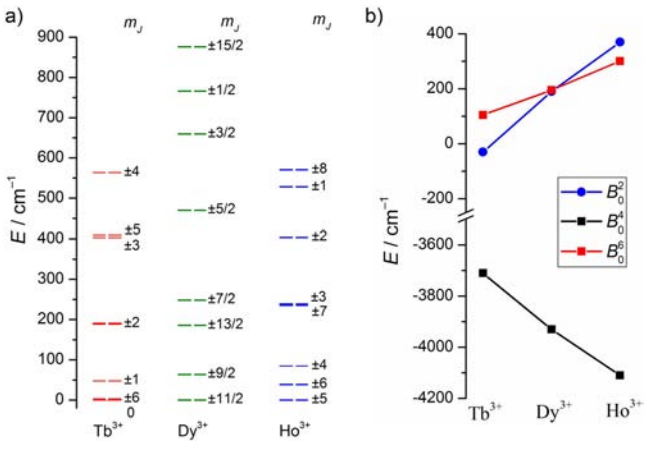

Figure 6. (a) Zero-field splitting of m_J substates of Ln^{3+} ions in compounds **3**, **1**, and **4**, based on ligand field parameters derived from least-squares fitting (Figure 6, Table 3). (b) Near-linear dependency of the Wyborne ligand field parameters as a function of the number of 4f electrons for f^8 (Tb^{3+}), f^9 (Dy^{3+}), and d^{10} (Ho^{3+}) based on least-squares fits for **3**, **1**, and **4**, respectively (lines: visual guides).

dx.doi.org/10.1021/ic302742u | Inorg. Chem. 2013, 52, 5035–5044

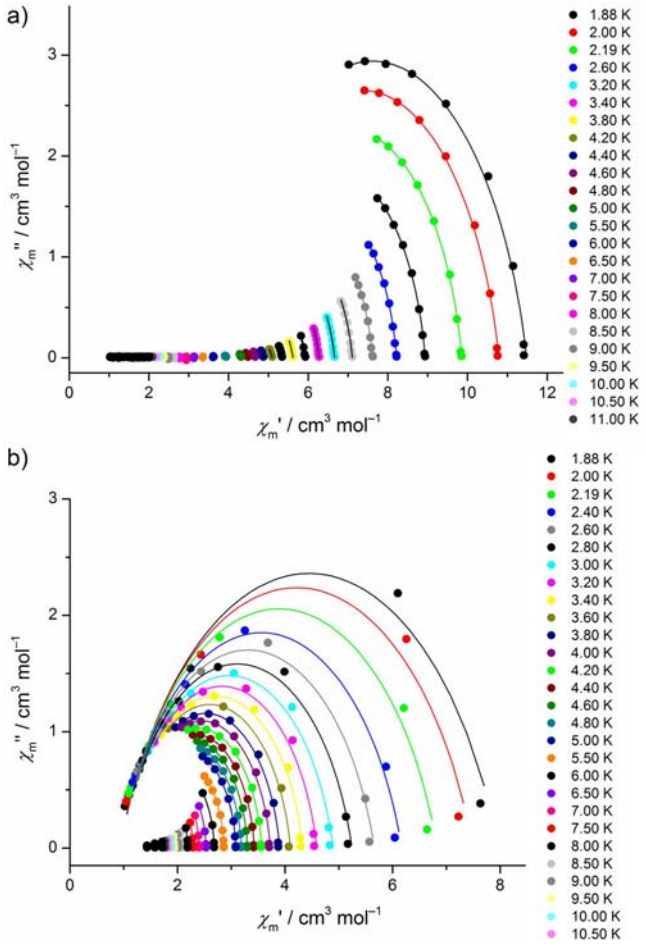

Figure 7. AC susceptibility components for $\{Mn_2Dy_2\}$-type compound **1** (a) and $\{Mn_2Tb_2\}$-type compound **3** (b). Experimental data: filled circles, fits to Cole−Cole equation: solid lines.

tunneling or Orbach-type relaxation and consequently decrease the effective relaxation barrier as well. Despite the slow magnetization relaxation, no hysteresis of the DC magnetization is observed down to 2.0 K.

Analogous to the structural comparison made vide supra, it is interesting to compare the magnetic behavior of the $\{Mn^{III}_2Ln^{III}_2\}$ family discussed here with related literature precedents. Among this family, magnetic studies on $Mn^{III}_2Ln_2(O)(Piv)_2(hep)_4(NO_3)_4$ (Figure 1a) (hep = 2-(2-hydroxyethyl)pyridine; Piv = pivalate) revealed that if Ln = Dy (III), Tb(III), or Ho(III), although slow magnetic relaxation is observed at low temperatures, maxima of the out-of-phase signal could not be detected precluding the determination of the energy barrier and the time constant.[21b] A similar observation has also been made for $[Mn^{III}_2Ln_2(OH)_2(NO_3)_4(hmp)_4(H_2O)_4](NO_3)_2$ (hmp = 2-hydroxymethylpyridine).[21c] However, for $[NMe_4]_2[Mn^{III}_2Dy^{III}_2(tmp)_2(O_2CMe_3)_4(NO_3)_4]$ (tmp = 1,1,1-tris(hydroxymethyl)propane) the estimated parameters ΔE = 15 K and $\tau_0 = 3.31 \times 10^{-7}$ s[21a] show (in comparison to **1**) that the overall molecular magnetic anisotropy of $\{Mn_2Dy_2\}$-type complexes can be altered considerably.

CONCLUSION

We have shown the successful design and assembly of a new family of tetranuclear, dicationic, heterometallic $\{Mn^{III}_2Ln^{III}_2\}$ complexes characterized by an arch-type topology. This was achieved by using an unsymmetrically substituted multisite coordinating ligand built on a vanillin platform. These centrosymmetric compounds contain the manganese ions in the periphery and the lanthanide ions in the center. While the geometry around the manganese(III) ion is octahedrally distorted, around the lanthanide ion a distorted elongated square-antiprismatic geometry is found. DC magnetic analysis reveals an overall antiferromagnetic interaction between the metal centers as well as pronounced single-ion effects in all four compounds. Despite the arched shape of the Mn−Ln−Ln−Mn backbone of these complexes, which effectively minimizes the net molecular magnetic anisotropy and possibly increase the probability of nonthermal relaxation mechanisms, AC magnetic studies reveal that compounds **1** and **3** retain sufficient anisotropy to exhibit slow relaxation of magnetization below 1.9 K with energy barriers of ΔE = 16.8 cm^{-1} (**1**) and ΔE = 33.8 cm^{-1} (**3**), and time constants $\tau_0 = 8.30 \times 10^{-9}$ s (**1**) and $\tau_0 = 1.63 \times 10^{-8}$ s (**3**). In this context, the significant zero-field splitting in Dy(III) and Tb(III) ions, in conjunction with the anisotropy of the Jahn−Teller-distorted Mn(III) ions, appears to be the dominant factor of the observed SMM behavior of **3** and **4**. Given the versatility of this family of $\{Mn_2Ln_2\}$-type compounds, we will further explore the option to modify the relative orientation of the ligand fields of both the Ln^{3+} and the Mn^{3+} centers via different chelating ligands to control the resulting molecular magnetic anisotropy.

ASSOCIATED CONTENT

Supporting Information

Crystallographic data in CIF format. Further details are given in Tables S1−S6 and Figures S1−S13. This material is available free of charge via the Internet at http://pubs.acs.org.

AUTHOR INFORMATION

Corresponding Author

*E-mail: vc@iitk.ac.in (V.C.), paul.koegerler@ac.rwth-aachen.de (P.K.).

Notes

The authors declare no competing financial interest.

ACKNOWLEDGMENTS

V.C. is thankful to the Department of Science and Technology, for a J. C. Bose fellowship. P.B. thanks Council of Scientific and Industrial Research, India for Senior Research Fellowship.

REFERENCES

(1) (a) Copÿret, C.; Chabanas, M.; Saint-Arroman, R. P.; Basset, J.-M. *Angew.Chem., Int. Ed.* **2003**, *42*, 156. (b) Shimizu, K.-I.; Shimura, K.; Nishimura, M.; Satsuma, A. *RSC Adv.* **2011**, *1*, 1310. (c) Kunz, S.; Hartl, K.; Nesselberger, M.; Schweinberger, F. F.; Kwon, G.; Hanzlik, M.; Mayrhofer, K. J. J.; Heiz, U.; Arenz, M. *Phys. Chem. Chem. Phys.* **2010**, *12*, 10288. (d) Mertens, P. G. N.; Corthals, S. L. F.; Ye, X.; Poelman, H.; Jacobs, P. A.; Sels, B. F.; Vankelecom, I. F. J.; De Vos, D. E. *J. Mol. Catal. A* **2009**, *313*, 14.

(2) (a) Mandal, S. K.; Roesky, H. W. *Acc. Chem. Res.* **2010**, *43*, 248. (b) Huang, J.; Fu, X.; Wang, G.; Geb, Y.; Miaoa, Q. *Catal. Sci. Technol.* **2012**, *2*, 1040. (c) Pignolet, L. H.; Aubart, M. A.; Craighead, K. L.; Gould, R. A.T.; Krogstad, D. A.; Wiley, J. S. *Coord. Chem. Rev.* **1995**, *143*, 219. (d) Sanchez-Delgado, R. A.; Puga, J.; Rosales, M. *J. Mol. Catal.* **1984**, *24*, 221. (e) Gates, B. C. *Chem. Rev.* **1995**, *95*, 511.

(3) (a) Eliseeva, S. V.; Bunzli, J.-C. G. *Chem. Soc. Rev.* **2010**, *39*, 189. (b) Ayyappan, P.; Evans, O. R.; Cui, Y.; Wheeler, K. A.; Lin, W. *Inorg.*

Chem. **2002**, *41*, 4978. (c) Wong, W.-Y.; Ho, C.-L. *Coord. Chem. Rev.* **2009**, *253*, 1709.
(4) (a) Carlin, R. L. *Magnetochemistry*; Springer-Verlag: Berlin, Germany, 1986. (b) Kahn, O. *Molecular Magnetism*; Wiley-VCH: Weinheim, Germany, 1993.
(5) (a) Gatteschi, D.; Fittipaldi, M.; Sangregorio, C.; Sorace, L. *Angew.Chem., Int. Ed.* **2012**, *51*, 4792. (b) Jeona, I.-R.; Clérac, R. *Dalton Trans.* **2012**, *41*, 9569. (c) Sessoli, R.; Powell, A. K. *Coord. Chem. Rev.* **2009**, *253*, 2328. (d) Murrie, M. *Chem. Soc. Rev.* **2010**, *39*, 1986. (e) Bagai, R.; Christou, G. *Chem. Soc. Rev.* **2009**, *38*, 1011. (f) Glaser, T. *Chem. Commun.* **2011**, *47*, 116. (g) Schray, D.; Abbas, G.; Lan, Y.; Mereacre, V.; Sundt, A.; Dreiser, J.; Waldmann, O.; Kostakis, G. E.; Anson, C. E.; Powell, A. K. *Angew. Chem., Int. Ed.* **2010**, *49*, 5185. (h) Sanz, S.; Ferreira, K.; McIntosh, R. D.; Dalgarno, S. J.; Brechin, E. K. *Chem. Commun.* **2011**, *47*, 9042. (i) Chandrasekhar, V.; Pandian, B. M.; Boomishankar, R.; Steiner, A.; Vittal, J. J.; Houri, A.; Clérac, R. *Inorg.Chem.* **2008**, *47*, 4918. (j) Feltham, H. L. C.; Lan, Y.; Klöwer, F.; Ungur, L.; Chibotaru, L. F.; Powell, A. K.; Brooker, S. *Chem.—Eur. J.* **2011**, *17*, 4362.
(6) (a) Caneschi, A.; Gatteschi, D.; Lalioti, N.; Sangregorio, C.; Sessoli, R.; Venturi, G.; Vindigni, A.; Rettori, A.; Pini, M. G.; Novak, M. A. *Angew. Chem., Int. Ed.* **2001**, *40*, 1760. (b) Harris, T. D.; Bennett, M. V.; Clerac, R.; Long, J. R. *J. Am. Chem. Soc.* **2010**, *132*, 3980. (c) Feng, X.; Harris, T. D.; Long, J. R. *Chem. Sci.* **2011**, *2*, 1688. (d) Miyasaka, H.; Madanbashi, T.; Saitoh, A.; Motokawa, N.; Ishikawa, R.; Yamashita, M.; Bahr, S.; Wernsdorfer, W.; Clerac, R. *Chem.—Eur. J.* **2012**, *18*, 3942. (e) Kajiwara, T.; Tanaka, H.; Nakano, M.; Takaishi, S.; Nakazawa, Y.; Yamashita, M. *Inorg. Chem.* **2010**, *49*, 8358. (f) Venkatakrishnan, T. S.; Sahoo, S.; Brefuel, N.; Duhayon, C.; Paulsen, C.; Barra, A.-L.; Ramasesha, S.; Sutter, J.-P. *J. Am. Chem. Soc.* **2010**, *132*, 6047. (g) Stamatatos, T. C.; Abboud, K. A.; Wernsdorfer, W.; Christou, G. *Inorg. Chem.* **2009**, *48*, 807. (h) Pardo, E.; Train, C.; Lescouezec, R.; Journaux, Y.; Pasan, J.; Ruiz-Perez, C.; Delgado, F. S.; Ruiz-Garcia, R.; Lloret, F.; Carley, P. *Chem. Commun.* **2010**, *46*, 2322. (i) Boeckmann, J.; Nather, C. *Chem. Commun.* **2011**, *47*, 7104.
(7) (a) Friedman, J. R.; Sarachik, M. P.; Tejada, J.; Ziolo, R. *Phys. Rev. Lett.* **1996**, *76*, 3830. (b) Wernsdorfer, W.; Aliaga-Alcalde, N.; Hendrickson, D. N.; Christou, G. *Nature* **2002**, *416*, 406. (c) Gatteschi, D.; Sessoli, R. *Angew. Chem., Int. Ed.* **2003**, *43*, 268.
(8) Wernsdorfer, W.; Sessoli, R. *Science* **1999**, *284*, 133.
(9) (a) Leuenberger, M. N.; Loss, D. *Nature* **2001**, *410*, 789. (b) Ardavan, A.; Rival, O.; Morton, J. J. L.; Blundell, S. J.; Tytyshkin, A. M.; Timco, G. A.; Winpenny, R. E. P. *Phys. Rev. Lett.* **2007**, *98*, 057201. (c) Stamp, P. C. E.; Gaita-Ariño, A. *J. Mater. Chem.* **2009**, *19*, 1718.
(10) (a) Candini, A.; Klyatskaya, S.; Ruben, M.; Wernsdorfer, W.; Affronte, M. *Nano Lett.* **2011**, *11*, 2634. (b) Ritter, S. K. *Chem. Eng. News.* **2004**, *82*, 29.
(11) (a) Karotsis, G.; Evangelisti, M.; Dalgarno, S. J.; Brechin, E. K. *Angew.Chem., Int. Ed.* **2009**, *48*, 9928. (b) Zheng, Y.-Z.; Evangelisti, M.; Tuna, F.; Winpenny, R. E. P. *J. Am. Chem. Soc.* **2012**, *134*, 1057. (c) Langley, S. K.; Chilton, N. F.; Moubaraki, B.; Hooper, T.; Brechin, E. K.; Evanghelisti, M.; Murray, K. S. *Chem. Sci.* **2011**, *2*, 1166. (d) Zheng, Y.-Z.; Evangelisti, M.; Winpenny, R. E. P. *Chem. Sci.* **2011**, *2*, 99. (e) Shaw, R.; Laye, R. H.; Jones, L. F.; Low, D. M.; Talbot-Eeckelaers, C.; Wei, Q.; Milios, C. J.; Teat, S.; Helliwell, M.; Raftery, J.; Evangelisti, M.; Affronte, M.; Collison, D.; Brechin, E. K.; McInnes, E. J. L. *Inorg. Chem.* **2007**, *46*, 4968. (f) Dinca, A. S.; Ghirri, A.; Madalan, A. M.; Affronte, M.; Andruh, M. *Inorg. Chem.* **2012**, *51*, 3935. (g) Evangelisti, M.; Brechin, E. K. *Dalton Trans.* **2010**, *39*, 4672.
(12) (a) Gatteschi, D.; Caneschi, A.; Pardi, L.; Sessoli, R. *Science* **1994**, *265*, 1054. (b) Hill, S.; Edwards, R. S.; Aliaga-Alcalde, N.; Christou, G. *Science* **2003**, *302*, 1015. (c) Gatteschi, D.; Sorace, L. J. *Solid State Chem.* **2001**, *159*, 253. (d) Sessoli, R.; Powell, A. K. *Coord. Chem. Rev.* **2009**, *253*, 2328−2341. (e) Neese, F. *J. Am. Chem. Soc.* **2006**, *128*, 10213. (f) Barra, A. L.; Gatteschi, D.; Sessoli, R. *Phys. Rev. B.* **1997**, *56*, 8192. (g) Aromi, O. G.; Brechin, E. K. *Struct. Bonding (Berlin)* **2006**, *122*, 1. (h) Inglis, R.; Jones, L. F.; Milios, C. J.; Datta, S.; Collins, A.; Parsons, S.; Wernsdorfer, W.; Hill, S.; Perlepes, S. P.; Piligkos, S.; Brechin, E. K. *Dalton Trans.* **2009**, 3403. (i) Wernsdorfer, W. *Adv. Chem. Phys.* **2001**, *118*, 99.
(13) (a) Vallejo, J.; Castro, I.; Ruiz-García, R.; Cano, J.; Julve, M.; Lloret, F.; De Munno, G.; Wernsdorfer, W.; Pardo, E. *J. Am. Chem. Soc.* **2012**, *134*, 15704. (b) Feng, X.; Liu, J.; Harris, T. D.; Hill, S.; Long, J. R. *J. Am. Chem. Soc.* **2012**, *134*, 7521. (c) Liu, J.-L.; Yuan, K.; Leng, J.-D.; Ungur, L.; Wernsdorfer, W.; Guo, F.-S.; Chibotaru, L. F.; Tong, M.-L. *Inorg. Chem.* **2012**, *51*, 8538.
(14) (a) Thomas, L.; Lionti, F.; Balou, R.; Gatteschi, D.; Sessoli, R.; Barbara, B. *Nature* **1996**, *383*, 145. (b) Mondal, K. C.; Sundt, A.; Lan, Y.; Kostakis, G. E.; Waldmann, O.; Ungur, L.; Chibotaru, L. F.; Anson, C. E.; Powell, A. K. *Angew. Chem., Int. Ed.* **2012**, *51*, 7550. (c) Rinehart, J. D.; Fang, M.; Evans, W. J.; Long, J. R. *Nat. Chem.* **2011**, *3*, 538. (d) Das, A.; Gieb, K.; Krupskaya, Y.; Demeshko, S.; Dechert, S.; Klingeler, R.; Kataev, V.; Büchner, B.; Müller, P.; Meyer, F. *J. Am. Chem. Soc.* **2011**, *133*, 3433. (e) Rinehart, J. D.; Fang, M.; Evans, W. J.; Long, J. R. *J. Am. Chem. Soc.* **2011**, *133*, 14236.
(15) Ako, A. M.; Hewitt, Mereacre, I. J. V.; Clerac, R.; Wernsdorfer, W.; Anson, C. E.; Powell, A. K. *Angew. Chem., Int. Ed.* **2006**, *45*, 4926.
(16) Ako, A. M.; Mereacre, V.; Clérac, R.; Wernsdorfer, W.; Hewitt, I. J.; Anson, C. E.; Powell, A. K. *Chem. Commun.* **2009**, 544.
(17) (a) Osa, S.; Kido, T.; Matsumoto, N.; Re, N.; Pochaba, A.; Mrozinski, J. *J. Am. Chem. Soc.* **2004**, *126*, 420. (b) Iasco, O.; Novitchi., G.; Jeanneau, E.; Wernsdorfer, W.; Luneau, D. *Inorg. Chem.* **2011**, *50*, 7373. (c) Baskar, V.; Gopal, K.; Helliwell, M.; Tuna, F.; Wernsdorfer, W.; Winpenny, R. E. P. *Dalton Trans.* **2010**, *39*, 4747. (d) Novitchi, G.; Wernsdorfer, W.; Chibotaru, L. F.; Costes, J. P.; Anson, C. E.; Powell, A. K. *Angew. Chem., Int. Ed.* **2009**, *48*, 1614. (e) Aronica, C.; Pilet, G.; Chastanet, G.; Wernsdorfer, W.; Jacquot, J. F.; Luneau, D. *Angew. Chem., Int. Ed.* **2006**, *45*, 4659. (f) Kajiwara, T.; Nakano, M.; Takaishi, S.; Yamashita, M. *Inorg. Chem.* **2008**, *47*, 8604. (g) Costes, J. P.; Vendier, L.; Wernsdorfer, W. *Dalton Trans.* **2010**, *39*, 4886. (h) Okazawa, A.; Nogami, T.; Nojiri, H.; Ishida, T. *Chem. Mater.* **2008**, *20*, 3110. (i) Feltham, H. L. C.; Clerac, R.; Powell, A. K.; Brooker, S. *Inorg. Chem.* **2011**, *50*, 4232. (j) Novitchi, G.; Costes, J. P.; Tuchagues, J. P.; Vendier, L.; Wernsdorfer, W. *New J. Chem.* **2008**, *32*, 197.
(18) (a) Papatriantafyllopoulou, C.; Stamatatos, T. C.; Efthymiou, C. G.; Cunha-Silva, L.; Paz, F. A. A.; Perlepes, S. P.; Christou, G. *Inorg. Chem.* **2010**, *49*, 9743. (b) Efthymiou, C. G.; Stamatatos, T. C.; Papatriantafyllopoulou, C.; Tasiopoulos, A. J.; Wernsdorfer, W.; Perlepes, S. P.; Christou, G. *Inorg. Chem.* **2010**, *49*, 9737. (c) Chandrasekhar, V.; Pandian, B. M.; Boomishankar, R.; Steiner, A.; Vittal, J. J.; Houri, A.; Clerac, R. *Inorg. Chem.* **2008**, *47*, 4918. (d) Xiong, K.; Wang, X.; Jiang, F.; Gai, Y.; Xu, W.; Su, K.; Li, X.; Yuan, D.; Hong, M. *Chem. Commun.* **2012**, *48*, 7456. (e) Mondal, K. C.; Kostakis, G. E.; Lan, Y.; Wernsdorfer, W.; Anson, C. E.; Powell, A. K. *Inorg. Chem.* **2011**, *50*, 11604. (f) Pointillart, F.; Bernot, K.; Sessoli, R.; Gatteschi, D. *Chem.—Eur. J.* **2007**, *13*, 1602. (g) Pasatoiu, T. D.; Sutter, J.-P.; Madalan, A. M.; Fellah, F. Z. C.; Duhayon, C.; Andruh, M. *Inorg. Chem.* **2011**, *50*, 5890.
(19) (a) Papatriantafyllopoulou, C.; Wernsdorfer, W.; Abboud, K. A.; Christou, G. *Inorg.Chem.* **2011**, *50*, 421. (b) Stamatatos, T. C.; Teat, S. J.; Wernsdorfer, W.; Christou, G. *Angew. Chem., Int. Ed.* **2009**, *48*, 521. (c) Mereacre, V. M.; Ako, A. M.; Clérac, R.; Wernsdorfer, W.; Filoti, G.; Bartolome, J.; Anson, C. E.; Powell, K. A. *J. Am. Chem. Soc.* **2007**, *129*, 9248. (d) Zaleski, C. M.; Depperman, E. C.; Kampf, J. W.; Kirk, M. L.; Pecoraro, V. L. *Angew. Chem., Int. Ed.* **2004**, *43*, 3912. (e) Mereacre, V.; Ako, A. M.; Clérac, R.; Wernsdorfer, W.; Hewitt, I. J.; Anson, C. E.; Powell, A. K. *Chem.—Eur. J.* **2008**, *14*, 3577. (f) Langley, S.; Moubaraki, B.; Murray, K. S. *Dalton Trans.* **2010**, *39*, 5066. (g) Mishra, A.; Wernsdorfer, W.; Abboud, K. A.; Christou, G. *J. Am. Chem. Soc.* **2004**, *126*, 15648.
(20) (a) Li, M.; Ako, A. M.; Lan, Y.; Wernsdorfer, W.; Buth, G.; Anson, C. E.; Powell, A. K.; Wang, Z.; Gao, S. *Dalton Trans.* **2010**, *39*, 3375. (b) Li, M.; Lan, Y.; Ako, A. M.; Wernsdorfer, W.; Anson, C. E.; Buth, G.; Powell, A. K.; Wang, Z.; Gao, S. *Inorg. Chem.* **2010**, *49*, 11587.

(21) (a) Mishra, A.; Wernsdorfer, W.; Parson, S.; Christou, G.; Brechin, E. *Chem. Commun.* **2005**, 2086. (b) Mereacre, V.; Lan, Y.; Clérac, R.; Ako, A. M.; Hewitt, I. J.; Wernsdorfer, W.; Buth, G.; Anson, C. E.; Powell, A. K. *Inorg. Chem.* **2010**, *49*, 5293. (c) Papatriantafyllopoulou, C.; Abboud, K. A.; Christou, G. *Inorg. Chem.* **2011**, *50*, 8959.
(22) (a) Shiga, T.; Onuki, T.; Matsumoto, T.; Nojiri, H.; Newton, G. N.; Hoshinoa, N.; Oshio, H. *Chem. Commun.* **2009**, 3568. (b) Akhtar, M. N.; Zheng, Y.-Z.; Lan, Y.; Mereacre, V.; Anson, C. E.; Powell, A. K. *Inorg. Chem.* **2009**, *48*, 3502. (c) Holynska, M.; Premuzic, D.; Jeon, I.-R.; Wernsdorfer, W.; Clerac, R.; Dehnen, S. *Chem.—Eur. J.* **2011**, *17*, 9605. (d) Liu, J.-L.; Guo, F.-S.; Meng, Z.-S.; Zheng, Y.-Z.; Leng, J.-D.; Tong, M.-L.; Ungur, L.; Chibotaru, L. F.; Heroux, K. J.; Hendrickson, D. N. *Chem. Sci.* **2011**, *2*, 1268.
(23) (a) Ke, H.; Zhao, L.; Guoa, Y.; Tang, J. *Dalton Trans.* **2012**, *41*, 2314. (b) Saha, A.; Thompson, M.; Abboud, K. A.; Wernsdorfer, W.; Christou, G. *Inorg. Chem.* **2011**, *50*, 10476.
(24) (a) Meng, Z.-S.; Liu, J.-L.; Leng, J.-D.; Guo, F.-S.; Tong, M.-L. *Polyhedron* **2011**, *30*, 3095. (b) Akhtar, M. N.; Lan, Y.; Mereacre, V.; Clerac, R.; Anson, C. E.; Powell, A. K. *Polyhedron* **2009**, *28*, 1698. (c) Chilton, N. F.; Langley, S. K.; Moubaraki, B.; Murray, K. S. *Chem. Commun.* **2010**, *46*, 7787.
(25) Chandrasekhar, V.; Pandian, B. M.; Boomishankar, R.; Steiner, A.; Clerac, R. *Dalton Trans.* **2008**, 5143.
(26) Wu, J.-Q.; Mu, J.-S.; Zhang, S.-W.; Li, Y.-S. *J. Polym. Sci., Part A: Polym. Chem.* **2010**, *48*, 1122.
(27) Furniss, B. S.; Hannaford, A. J.; Smith, P. W. G.; Tatchell, A. R. *Vogel's Text book of Practical Organic Chemistry*, 5th ed.; ELBS, Longman: London, U.K., 1989.
(28) (a) *SMART & SAINT, Software Reference manuals*, version 6.45; Bruker Analytical X-ray Systems, Inc.: Madison, WI, 2003. (b) Sheldrick, G. M. *SADABS, a software for empirical absorption correction*, version 2.05; University of Göttingen: Göttingen, Germany, 2002. (c) *SHELXTL Reference Manual*, version 6.1; Bruker Analytical X-ray Systems, Inc.: Madison, WI, 2000. (d) Sheldrick, G. M. *SHELXT*, version 6.12; Bruker AXS Inc.: Madison, WI, 2001. (e) Sheldrick, G. M. *SHELXL97, Program for Crystal Structure Refinement*; University of Göttingen: Göttingen, Germany, 1997. (f) Brandenburg, K. *Diamond*, v3.1e; Crystal Impact GbR: Bonn, Germany, 2005.
(29) Speldrich, M.; Schilder, H.; Lueken, H.; Kögerler, P. *Isr. J. Chem.* **2011**, *51*, 215.
(30) (a) Brown, I. D.; Wu, K. K. *Acta Crystallogr.* **1976**, *B32*, 1957. (b) Liu, W.; Thorp, H. H. *Inorg. Chem.* **1993**, *32*, 4102.
(31) (a) Roy, L. E.; Hughbanks, T. *J. Am. Chem. Soc.* **2006**, *128*, 568. (b) Costes, J. P.; Dupuis, A.; Laurent, J. P. *Inorg. Chim. Acta* **1998**, *268*, 125.
(32) (a) Cole, K. S.; Cole, R. H. *J. Chem. Phys.* **1941**, *9*, 341. (b) Dekker, C.; Arts, A. F. M.; Wijn, H. W.; van Duyneveldt, A. J.; Mydosh, J. A. *Phys. Rev. B* **1989**, *40*, 11243.